

NPS ARCHIVE  
1959  
GARNER, W.

A MASER STABILIZED K-BAND  
SIGNAL GENERATOR

WILLIAM G. GARNER

Library  
U. S. Naval Postgraduate School  
Monterey, California









A MASER STABILIZED  
K-BAND SIGNAL GENERATOR

\* \* \* \* \*

William G. Garner





A MASER STABILIZED  
K-BAND SIGNAL GENERATOR

by

William G. Garner

Captain, United States Marine Corps

Submitted in partial fulfillment of  
the requirements for the degree of

MASTER OF SCIENCE  
IN  
ENGINEERING ELECTRONICS

United States Naval Postgraduate School  
Monterey, California

1 9 5 9

IPS HKTIVE

959

ARNER, W.

~~CONFIDENTIAL~~

A MASER STABILIZED  
K-BAND SIGNAL GENERATOR

by

William G. Garner

This work is accepted as fulfilling  
the thesis requirements for the degree of  
MASTER OF SCIENCE

IN

ENGINEERING ELECTRONICS

from the

United States Naval Postgraduate School



## ABSTRACT

A stable K-band signal generator which uses an ammonia beam maser as a reference is described. The signal generator has a stability of one part in  $10^7$  over periods of one hour or more and one part in  $10^8$  for shorter periods. Improved circuitry in the i-f portions of the stabilization loop would give stabilities of one part in  $10^9$  or better. The tuning range of the signal generator is from two megacycles per second below the reference signal to two megacycles per second above the reference. A technique for Q measurements on high Q cavities using the signal generator is discussed and the results of three such measurements are reported. A method for measuring the gain of a maser amplifier to within 0.5 db using the signal generator is presented and some preliminary results are reported. Several other applications of the signal generator are considered.

The writer wishes to express his gratitude to Professor Carl E. Menneken of the United States Naval Postgraduate School for his encouragement in preparing for this work and for his constructive criticism while preparing the manuscript. The writer also wishes to thank the Molecular Beams Group of Hughes Research Laboratories for their help in performing the experimental work. The writer is particularly grateful to Dr. Malcolm L. Stitch of Hughes Research Laboratories for suggesting and supervising the experimental work and to Dr. John Walsh for the use of his phase lock loop and for his help with the i-f circuitry.



## TABLE OF CONTENTS

Section	Title	Page
1.	Introduction	1
2.	Theory of Maser Operation	3
3.	Klystron Stabilization	9
4.	Construction and Testing of the Stabilized K-Band Signal Generator	16
5.	Cavity Measurements	26
6.	Maser Gain Measurements Using the Stabilized Signal Generator	32
7.	Conclusions	36
8.	Bibliography	<del>45</del> 43





# LIST OF ILLUSTRATIONS

Figure		Page
1.	Model of the Ammonia Molecule Showing the Pyramidal Structure	4
2.	Stark Effect in the Ammonia Molecule	4
3.	Cross Section of a Four Pole Focuser Showing the Electric Field Configuration	7
4.	Diagram of a Beam Maser Showing the Important Parts	7
5.	Simplified Block Diagram of a Pound Stabilizer Circuit Using an Ammonia Absorption Cell	11
6.	Simplified Block Diagram of a Phase Detector Loop	11
7.	Schematic of the 21mcs Phase Detector	12
8.	A Method for Obtaining $f_0 + \delta$ Using Two Phase Lock Loops	15
9.	Schematic of 18 - 23mcs Variable Frequency Oscillator	17
10.	Single Phase Lock Loop for Obtaining $f_0 + \delta$	20
11.	Heterodyne Method for Obtaining $f_0 + \delta$	23
12.	Block Diagram of Apparatus Used for Q Measurements	30
13.	Equivalent Circuit for a Microwave Cavity	30
14.	Plot of VSWR Versus Frequency for Determining the Loaded Q of an Experimental Cavity	31
15.	Block Diagram of Gain Measuring Apparatus	35
16.	A Method for Obtaining a Stable 8000mcs Oscillator	38
17.	A Maser Stabilized C. - W Radar	40
18.	Block Diagram of Modified Dicke Radiometer	44



## 1. Introduction

The maser is a relatively new device first developed by Gordon, Zeiger, and Townes at the Columbia Radiation Laboratory in 1955.<sup>1</sup> The term maser was coined at this time as an acronym for "microwave amplification by stimulated emission of radiation" and is now used to describe molecular beam and solid state devices. The more recent parametric amplifiers are frequently grouped with masers although they operate on a different principle.

Since masers are molecular devices rather than electronic, the absence of electric charge and its consequent shot noise results in very low noise figures. As a result of this low noise figure, masers have attracted a lot of attention for possible use as preamplifiers in ultra sensitive receivers such as those used in radio astronomy. Solid state masers have been developed with gains of 20 to 30 decibels with a system noise temperature of 25 degrees Kelvin or less.

In spite of this very desirable noise figure, the ammonia beam masers have limitations that restricts their usefulness as preamplifiers to certain special applications. These limitations are brought about by their inherent narrow bandwidth and their lack of tunability. Ammonia beam masers have a half-power bandwidth of about one kilocycle per second at a fixed frequency of 23,870 megacycles per second. Fortunately solid state masers have much better bandwidths which may be as high as several megacycles per second at X-band and they may be "tuned" over a considerable band of frequencies.

The first masers were of the ammonia beam variety and were operated as oscillators rather than amplifiers. When operated in this manner,



they have one very interesting and useful property, namely that they are extremely stable. The fact that they are not "tunable" as amplifiers, since their frequency is determined by internal molecular constants, makes them invaluable as fixed frequency standards of high stability. Short time stabilities of a few parts in  $10^{13}$  and long time stabilities of one part in  $10^{11}$  (this is comparable to a clock that gains or loses one second in 3000 years) have been reported using ammonia beams. With these almost unbelievable stabilities available, the logical thing to do was to develop some new frequency standards based upon the maser oscillator as a reference and a great deal of effort has gone in that direction. Recently, other standards have appeared that may be potentially more stable than the beam maser<sup>2</sup> but these are generally more complex than masers which limits their application.

An ammonia beam maser oscillator unlike many of the other standards is an active device and has a useable output of approximately -70 dbm. Since it is an active device the maser is more versatile than most of the other types of frequency standards. Because of this small output power, various techniques have been developed to obtain stable signals at higher power levels using the maser as a reference. This paper is concerned with such a technique to stabilize a reflex klystron to a maser and some applications of this stabilized signal.





## 2. Theory of Maser Operation

From a macroscopic point of view, the theory of operation of a maser is relatively simple and straight forward although it becomes somewhat involved if all the quantum mechanical details are examined. For the purposes of this paper, it will not be necessary to go into all the minute ramifications of the theory. The remarks to follow are concerned with beam masers although the basic principles are the same for solid state masers. These differ primarily in the method of obtaining an excess of molecules in the upper energy state.

Virtually all beam masers in existence today use the inversion of the  $J = 3, K = 3$  line of the ammonia molecule, although Higa<sup>3</sup> and others have used the inversion of the 2,2 line and work is in progress in several places using other gases such as HCN. The ammonia molecule can be visualized as a pyramid with the three hydrogen atoms forming the base and the nitrogen atom forming the apex as shown in Figure 1. The nitrogen atom can be either above or below the base. Owing to a complex quantum mechanical effect called tunneling, the molecule can vibrate between these two positions at a characteristic resonance frequency. This resonance can accompany either the absorption or emission of an appropriate amount of energy. After absorption the molecule is said to be in an excited state corresponding to an upper energy level. After emission the molecule is said to be in the ground state corresponding to a lower energy level. These are called inversion levels of the ammonia molecule.

At or near room temperature the two inversion levels reach an equilibrium condition such that there are approximately 1/250 more molecules





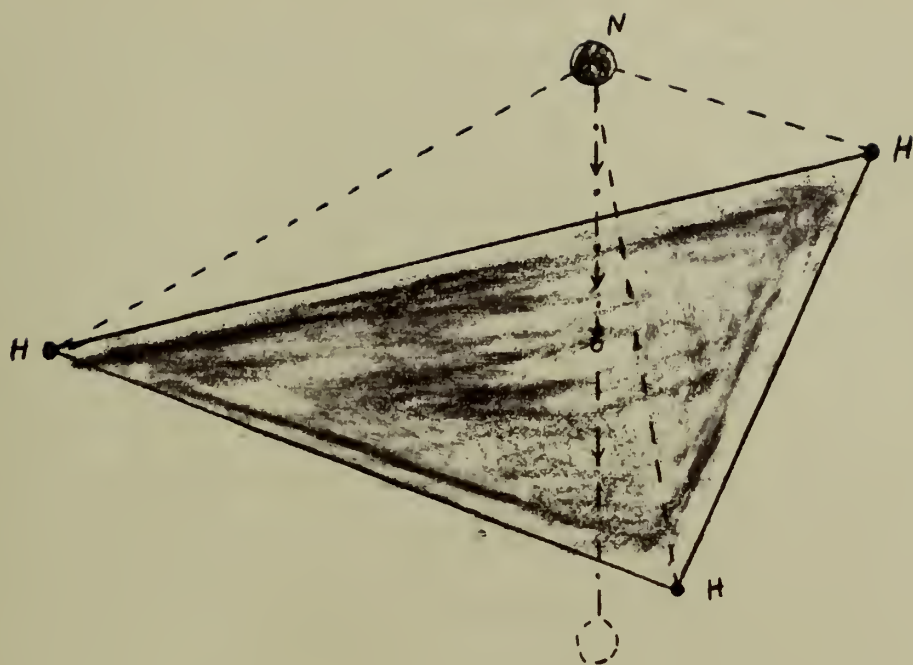


Figure 1. Model of the ammonia molecule showing the pyramidal structure.

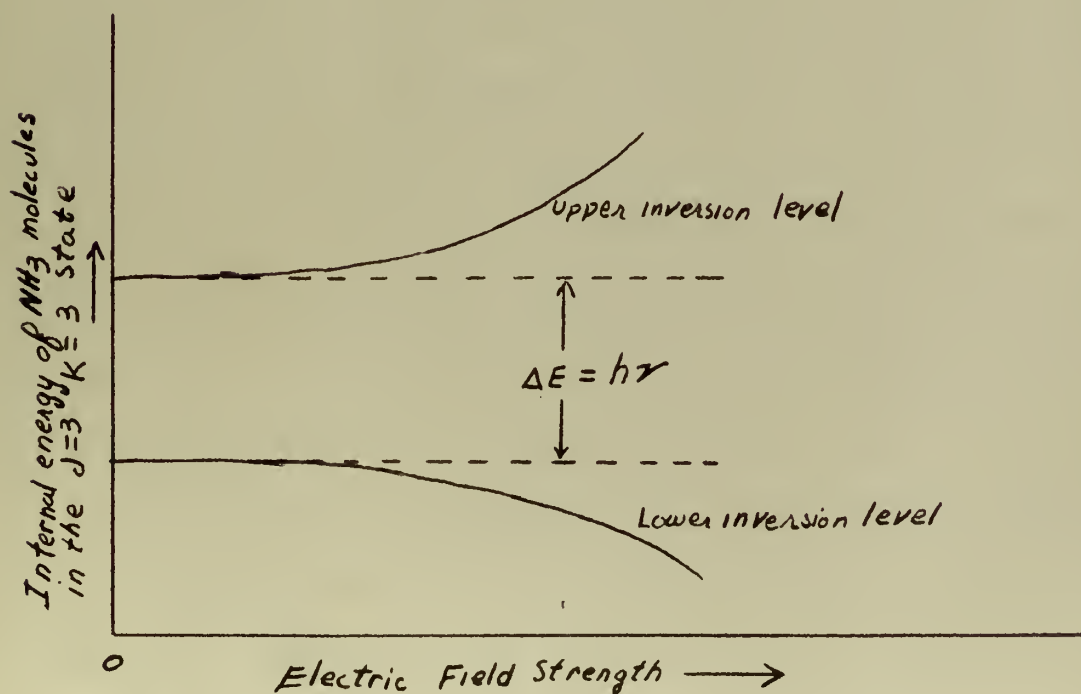


Figure 2. Stark Effect in the ammonia molecule.



in the lower level than in the upper. In this condition, molecules in the lower level are being thermally excited to the upper level and simultaneously those in the upper level are thermally stimulated to the lower level. These transitions to the lower level are accompanied by an emission of electromagnetic energy of frequency given by  $f = \Delta E/h$  where  $f = 23,870.131$  megacycles per second for the 3,3 inversion and  $f = 23,722.634$  megacycles per second for the 2,2 inversion.  $\Delta E$  is the energy separation between levels and  $h$  is Planck's constant. The average spontaneous decay time from the higher to the lower level in the absence of thermal stimulation is approximately three hours.

Consider now a beam of molecules that are all in the upper inversion level. If this beam is perturbed by an electromagnetic field at a frequency corresponding to the transition frequency, it will be stimulated into emission and will give up its energy and radiate in phase with the field rather than randomly over a period of time. If this beam of molecules in the upper level is allowed to pass through a cavity tuned to the resonance frequency of the molecular transition, a regenerative loop will be formed with the beam forming its own perturbing field. Oscillations will be sustained as long as the beam is supplying enough energy to overcome the ohmic losses in the walls and any energy that is coupled out of the cavity. Nonlinearities will prevent the oscillations from exceeding about  $10^{-10}$  watts where saturation occurs.

Figure 4 gives a block diagram of a beam maser showing the formation of the beam, the focuser for separating the levels, the cavity, and the waveguide for coupling the energy out of the cavity. The entire system is in a vacuum of about  $5 \times 10^{-6}$  millimeters of mercury.



The beam is formed by allowing ammonia gas at a few microns pressure to effuse through a short section of nozzles such as a Varian klystron grid into the vacuum system. The beam that emerges from the nozzles is collimated and flows through the center of the focuser electrodes where the level separation takes place. The beam leaving the focuser electrodes will have an excess of molecules in the upper level which will then enter the cavity where they will be stimulated into emission.

Figure 2 is an energy versus electric field diagram for the two levels of the 3,3 line for ammonia showing the Stark effect. Note that as the electric field increases, the upper level gains energy while the lower level loses energy. This suggests that a non-uniform electric field could be used as a method for separating the two inversion levels. In such a field, the lower level molecules will be attracted to the strongest part of the field and the upper levels will be attracted to the weaker part of the field. Figure 3 shows a simple focuser similar to the one used in the earlier masers for separating the two inversion levels. The upper and lower electrodes are at a high potential while the other two electrodes are grounded giving a field configuration as shown in Figure 3. Thus, the field is zero in the center and increases in magnitude in the radial direction. A beam of ammonia molecules flowing perpendicular to a field of this sort will experience a focusing action which will pull the lower level molecules to the outside of the beam and attract the upper level molecules to the center of the beam. The dotted lines in Figure 4 show this focusing action.





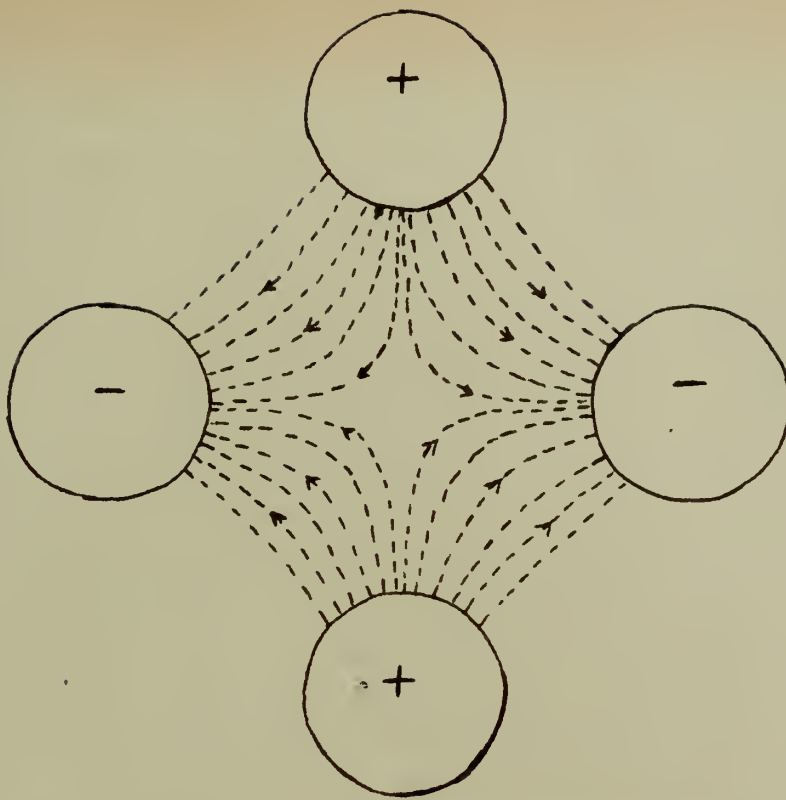


Figure 3. Cross section of a four pole focuser showing the electric field configuration.

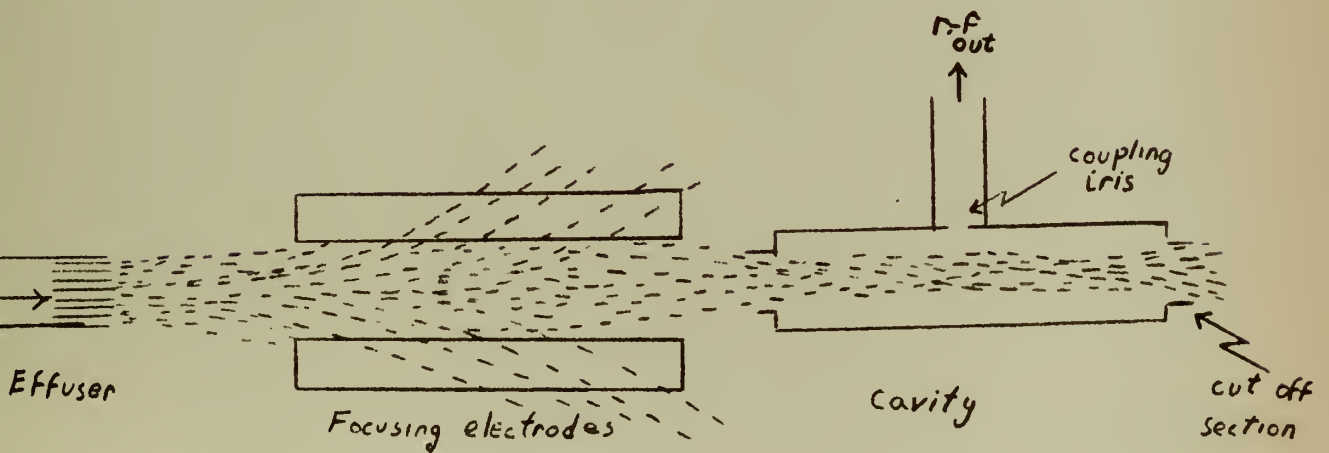


Figure 4. Diagram of a beam maser showing the important parts.





The cavity of a maser is a very important and critical component and requires considerable care in its design. It is important that its diameter is large enough to allow the beam to enter and have sufficient length to allow a long interaction time as the beam drifts through. A cylindrical cavity operating in the  $TE_{01n}$  or the  $TM_{01n}$  mode meets these conditions and will give a diameter of about 0.4 inches and a length of 5 to 6 inches. For maximum efficiency, it is necessary that the cavity operate in the fundamental mode or the first mode in some cases. As mentioned earlier, it is necessary that the beam supply sufficient energy to overcome the losses in the walls which requires that the  $Q$  of the cavity be high to minimize the starting beam current. A typical cavity would have an unloaded  $Q$  of 10,000, operate in the  $TM_{011}$  mode and have a small iris in the center for coupling energy out.

For further information on the theory and construction of beam masers there are several good references available. Damon<sup>4</sup> gives a very basic presentation of beam and solid state maser theory and is very easy reading. Lyons<sup>2</sup> also gives a simplified picture of maser theory as well as some of the basic theory behind other atomic clocks. Wittke<sup>5</sup> goes into a little more detail concerning the theory of beam and solid state masers and also discusses a new method of state separation suggested by Dicke at Princeton. Details of maser construction can be found in articles by Higa<sup>3</sup>, Helmer<sup>6</sup>, and Gordon<sup>1</sup>. Helmer's article also gives a very complete discussion of the theory behind maser operation. More articles will be found in the Bibliography Section and a very complete set of references on masers and parametric amplifiers will be found at the conclusion of Heffners paper.<sup>7</sup>



### 3. Klystron Stabilization

The maser is a relatively new device but the use of the same transition in ammonia dates back many years. In 1933 Wright and Randall<sup>8</sup> made a spectroscopic observation that indicated a transition around 1.25 centimeters in ammonia. The following year Cleeton and Williams<sup>9</sup> demonstrated that there was a microwave absorption due to ammonia using a large bag filled with ammonia gas and passing a microwave signal through the bag and noting the diminution of the signal. In 1946 R. V. Pound developed a method for stabilizing a klystron by using these absorption properties.<sup>10</sup> Figure 5 is a block diagram of the Pound frequency stabilization loop. A sample of the r-f energy from the klystron is admitted into a section of waveguide several meters long filled with ammonia gas at a pressure of a few microns. When the klystron is right at the frequency of the ammonia absorption line, there will be a sizeable attenuation of the signal as it propagates down the waveguide and the output of the discriminator will be a minimum. If the klystron drifts slightly off frequency the attenuation due to ammonia absorption will be less and the output of the discriminator will increase. If this detected signal is amplified and added to the repeller voltage on the klystron with the proper polarity this will tend to bring the klystron back to the proper frequency. Due to the use of waveguide operating well below cut-off wavelength necessary for the absorption cell there is considerable Doppler broadening. This along with pressure broadening due to collisions in a gas at sufficiently high pressure and other factors limits the stability of a loop such as this to about one part in  $10^7$ . Several variations on this basic idea have been suggested and tried but



these have resulted in only slight improvements in stability.<sup>11,12,13,14</sup>

With the advent of the ammonia maser as a frequency standard, new methods for klystron stabilization became possible. Peter and Strandberg<sup>15</sup> suggested a method for phase stabilization which was readily adaptable to klystron oscillators using the maser as a reference. Davis<sup>16</sup> made some modifications to the phase detector of Peter and Strandberg and added an integrating filter which allowed the system to correct for low frequency deviations more effectively. Using a loop as shown in Figure 6, Davis succeeded in phase stabilizing a reflex klystron to a maser oscillator. Figure 7 is a circuit diagram of the phase detector and integrating filter as further modified for experimental work carried out by the writer at Hughes Research Laboratories.

Due to the low level of the maser signal, it is necessary to use a very high gain i-f amplifier in order to operate the phase detector at a high level and avoid d-c amplifiers as was necessary in the Pound method. An amplifier with a gain of about 100 decibels is necessary to operate the phase detector at a level of from one to two volts. Typical K-band klystrons have an electronic tuning sensitivity of about two megacycles per volt which indicates that the loop will correct for drifts in frequency of from two to four megacycles on either side of the center frequency. Since the phase detector is in series with the repeller lead, it is necessary that it be well insulated as the repeller voltages in use on K-band klystrons range from one hundred to four hundred volts which is in turn impressed upon a beam voltage of from 350 to 1800 volts giving a total voltage of up to 2300 volts with respect to ground if the anode is grounded.





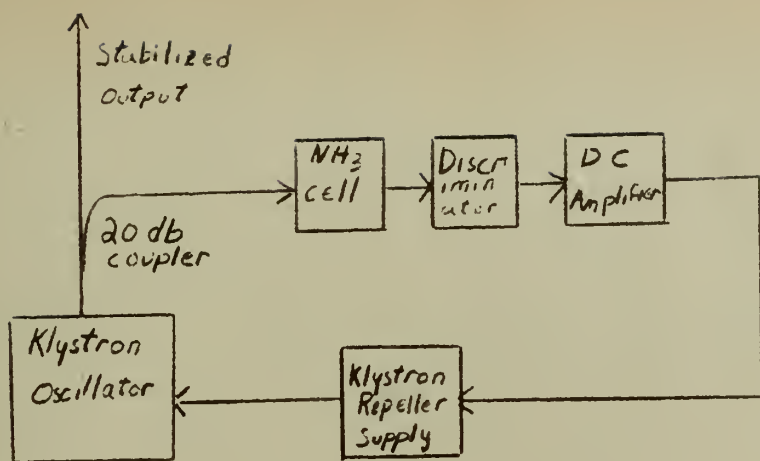


Figure 5 Simplified block diagram of a Pound stabilizer circuit using an ammonia absorption cell.

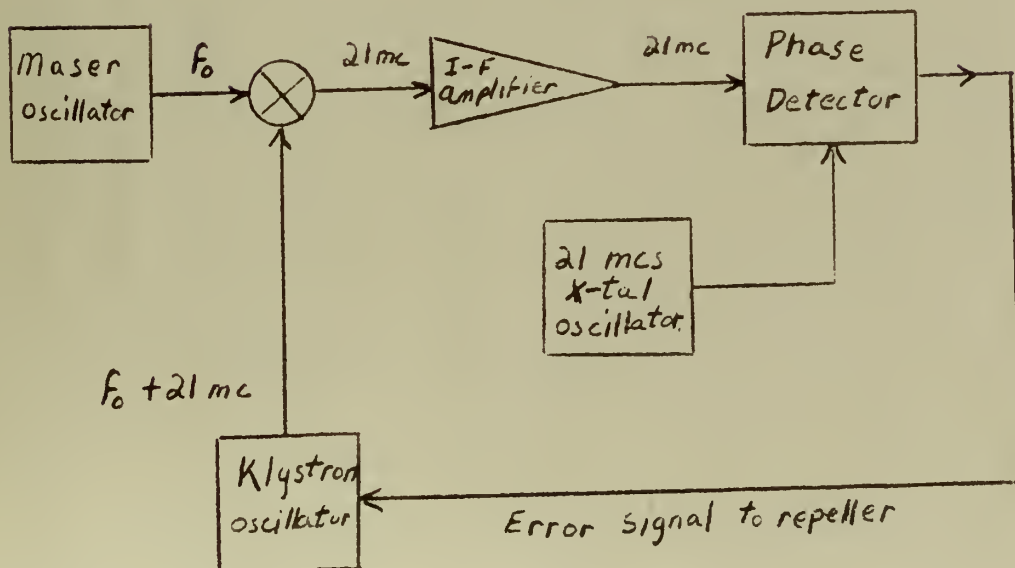


Figure 6. Simplified block diagram of phase detector loop.





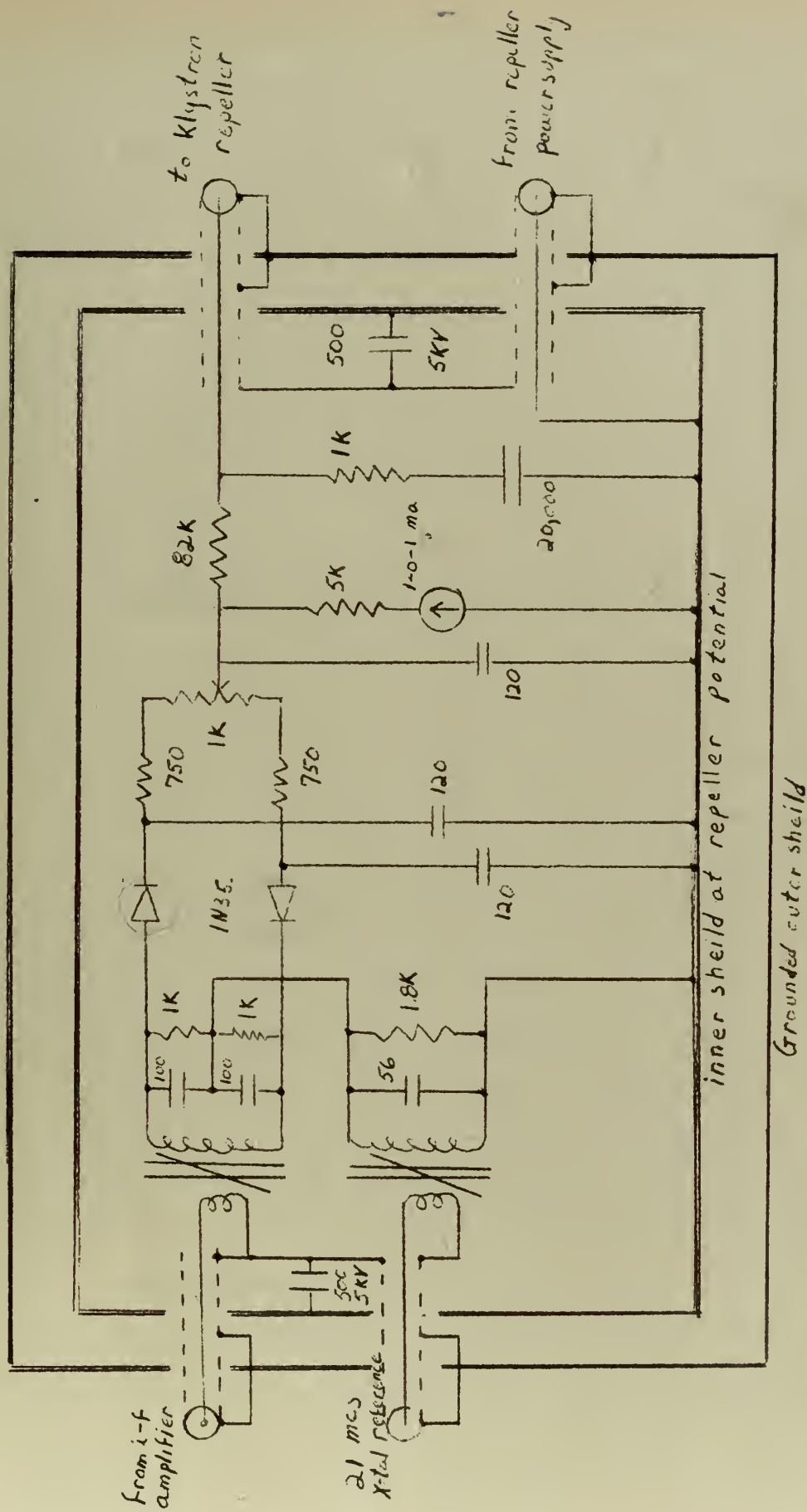


Figure 7. Schematic of the 21 mcs phase detector and integrating filter.



The stability of a phase lock loop of this nature is generally limited by the stability of the low-frequency reference oscillator which is normally stable to a few parts in  $10^7$  at best. Since the phase detector loop will follow the 21 megacycles per second reference oscillator cycle by cycle, the frequency uncertainty will be the sum of the maser uncertainty and the 21 megacycles per second oscillator uncertainty. Using reasonable care it is possible to achieve stabilities of a few parts in  $10^{10}$  over short periods of time with an ammonia beam maser. At 24,000 megacycles per second this gives an uncertainty in the output frequency of approximately three cycles per second. The crystal oscillator used as the reference signal by the writer had a stability of about one part in  $10^6$  which would give an uncertainty of about 21 cycles per second at 21 megacycles per second. Using these figures, it is apparent that in the worst case the klystron would have an uncertainty in its output of up to 24 cycles per second at 24 kilomegacycles per second or a stability of about one part in  $10^9$ . There are two difficulties with a system of this sort; it is fixed in frequency and it is displaced from the maser frequency by the amount of the reference signal which was 21 megacycles per second in this case.

It was suggested by Dr. Malcolm L. Stitch\* that some method be devised whereby a klystron could be stabilized at maser frequency with an arrangement in the loop whereby the stabilized signal could be tuned over a limited frequency range above and below the maser frequency  $f_0$ . The reasons for desiring a system of this sort will be discussed later in the paper. The requirements for the system were that it have a power

\* Atomic Physics Department, Hughes Research Laboratories, Culver City, California



output of one tenth of a milliwatt or greater over the tuning range. This was to be at least one megacycle above and below the maser frequency. A method for precisely determining the frequency of the K-band signal was also required.

Several approaches to the problem were considered that differed in complexity and ease of operation. Figure 8 shows the first method considered which was felt to be the most reliable of all the systems but also the most complex. It is essentially a phase lock loop that is used to drive another phase lock loop and as such requires two klystrons, two phase detectors, two i-f strips and two low-frequency oscillators. Figure 10 shows a system that is a simple phase lock loop with an additional low frequency oscillator and mixer in the local oscillator arm. Due to its simplicity, it was felt that this would be the easiest system to attempt first. In the event this system did not function properly the system of Figure 11 would be the next to be tried even though it would not have the power output of the other systems. It was felt that a lower output power was more desirable than the added complexity of the system of Figure 8 which would be used if the other two systems did not work. This last system was not attempted as the system of Figure 11 was operated successfully.



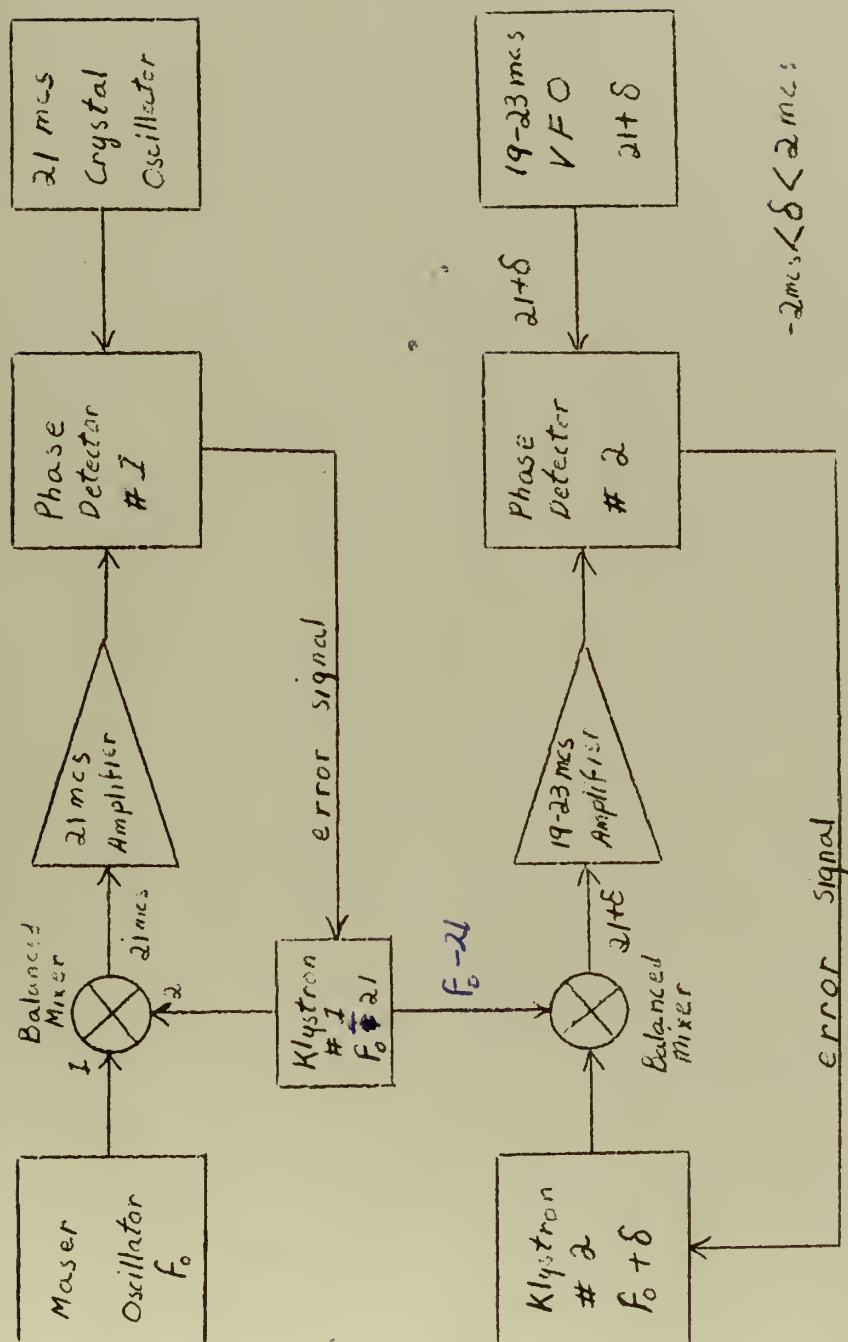


Figure 8. Method for obtaining  $f_0 + \delta$  using two phase lock loops.





#### 4. Construction and Testing of the Stabilized K-Band Signal Generator

The first task was to construct a variable frequency oscillator to be used in the loop of any of the systems of Figures 8, 10 and 11. Due to time limitations it was decided that a relatively simple oscillator would be sufficient to demonstrate the feasibility of the system if it had a short time stability of one kilocycle per second per second or better. The circuit used was a modified Colpitts or Clapp oscillator followed by a cathode follower and one stage of amplification as shown in Figure 9. After an initial warm up of one hour the oscillator was found to have a frequency drift of less than 50 cycles per second per minute. The tuning range was from 19 to 23 megacycles per second with an output of approximately five volts r.m.s. across a 93 ohm load over the tuning range. The fine frequency control allowed the oscillator to be set to within 100 cycles of any frequency with relative ease.

After completion of the low-frequency variable frequency oscillator, it was substituted for the crystal oscillator in the phase lock loop of Figure 6 in order to check out the system bandwidths. Using this set up it was found that the klystron could be tuned over the entire frequency range of  $(f_0 + 19)$  to  $(f_0 + 23)$  megacycles per second and remain locked to the maser reference which indicated that the bandwidths of the phase detector and i-f amplifier were sufficient to use without any further modifications. Using this system, the  $Q$  of an experimental maser cavity was determined as will be described in Section 5.

The circuit of Figure 10 was assembled in an attempt to stabilize the klystron at or near the maser frequency with no success. It was first thought that the system was working somewhat intermittently as







it appeared to phase lock occasionally but would not stay locked as the low-frequency reference was tuned. In the belief that the system was working marginally, a great deal of effort went into carefully peaking up the two balanced mixers and filter but this did not solve the problem. Confronted with these facts a more careful analysis of the loop was made to determine the cause of the apparent locking.

Before going into the analysis of the loop it might be well to mention briefly some of the problems that one is confronted with when working at K-band. Most of the problems revolve around the state of the art in the development of components and equipment which a person with experience at X-band or lower frequencies may not appreciate. Little or no development has gone into the development of radar at these frequencies since World War II because of the severe absorption of radiation due to water vapor and oxygen. As a result, components that are readily available at lower frequencies are not available at K-band or they are unreasonably expensive due to development costs with a small market for them after development. As a result of this, many of the components must be fabricated in the laboratories that are using them. This is always time consuming and frequently not too successful. Another difficulty at K-band is the 1N26 crystal which is noisy, has large conversion losses, and will handle only limited amounts of power. Until very recently, this was the only crystal available for use at K-band. Sylvania has developed a new K-band crystal, the 1N26A, that is reported to have improved power handling capabilities with smaller conversion losses and less noise.

A careful analysis of the problem revealed that two things were





responsible for most of the trouble in the loop of Figure 10. The first of these was the lack of a modulator as was required in this system. Not having a balanced modulator designed as such, a balanced mixer was used in reverse. This worked reasonably well considering that it was designed to mix two r-f signals and take out an i-f signal. Using the mixer as a modulator and checking the output on a spectrum analyser it was observed that the two sidebands were of approximately equal amplitude with the carrier suppressed by approximately 20 db. Conversion losses in the modulator were such that when driving the crystals with maximum allowable power, no more than one half milliwatt in each sideband could be obtained. The next difficulty was due to the filter used after the modulator to further attenuate the carrier and the other sideband. The filter was a transmission cavity with an additional iris to vary the bandwidth. The insertion loss was from three to ten decibels depending upon the bandwidth setting. This filter gave an additional 20 db of attenuation to the carrier and about 30 db to the other sideband but reduced the power out of the filter to one quarter milliwatt maximum at the desired frequency. The optimum power into the mixer for best signal to noise ratio is about one milliwatt but it was found that the mixer would operate reasonably well down to 0.2 milliwatts where the signal to noise ratio starts to drop off rapidly.



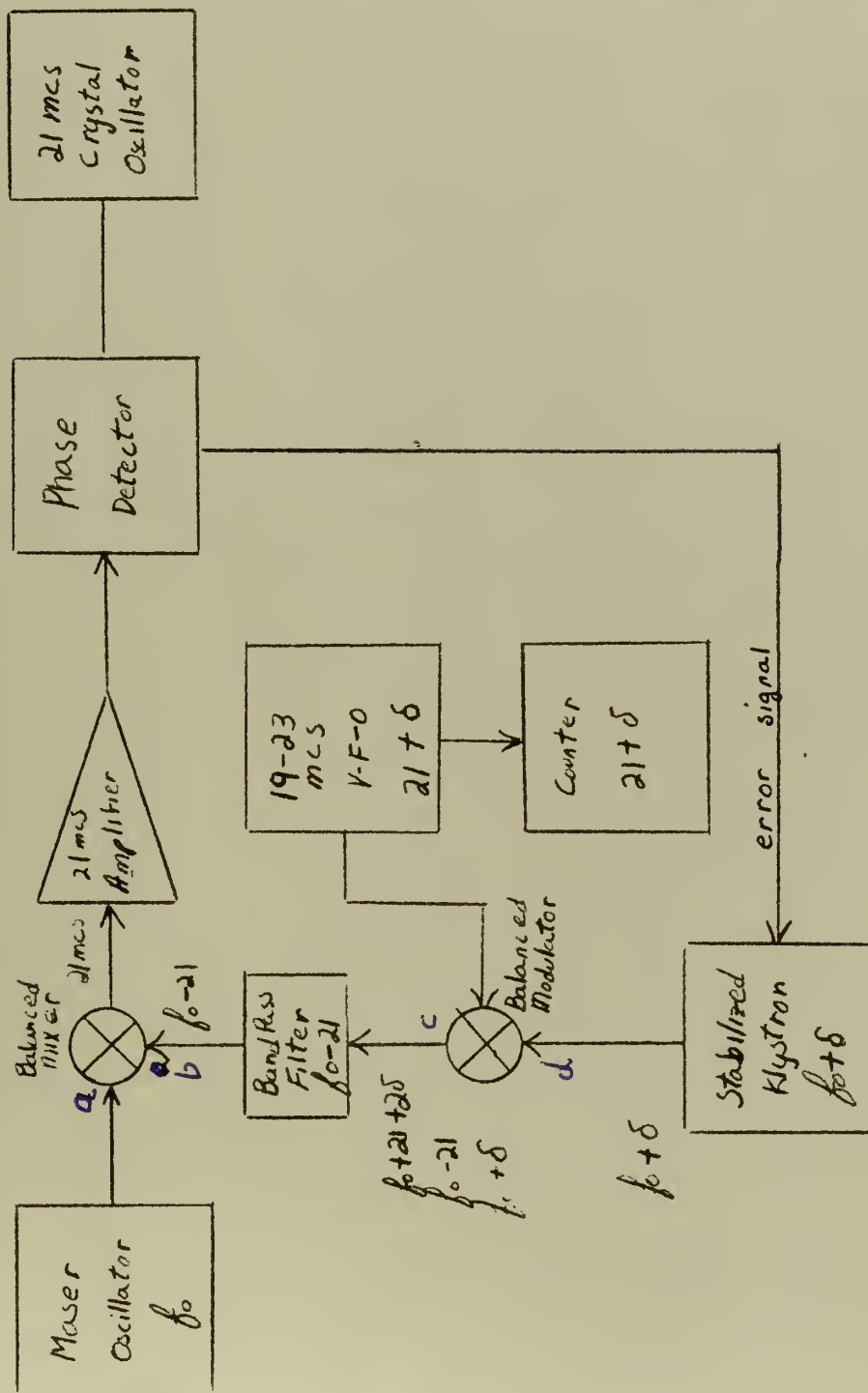


Figure 10. Single phase lock loop for obtaining  $f_0 + \delta$ .



TABLE I

	$f_o$	$f_o + \delta$	$f_o - 21$	$f_o + 21 + 2\delta$
Maser Output	-70 dbm	-	-	-
Mixer Input a	-70 dbm	-63 dbm	-	-53 dbm
Mixer Input b	-	-43 dbm	-6 dbm	-33 dbm
Modulator Output c	-	-23 dbm	-3 dbm	-3 dbm
Modulator Input d	-	3 dbm	-	-

Tabulation of carrier and sideband powers at various points in Figure 10.

Table I is a tabulation of powers at various points throughout the system for the signals of interest. It will be noted that the carrier power at the b input to the balanced mixer is about -43 dbm. The balanced mixer number one will give another 20 db of effective attenuation to the carrier for mixing purposes which puts it at about -63 dbm. The maser that was used for the reference in the loop under test had a power output of roughly -70 dbm when properly tuned. For reliable operation there should be no signals present that are comparable in frequency and power to the maser signal in arm <sup>a</sup> of the crystal mixer. Unless each and every portion of the loop was very carefully and precisely tuned, the carrier signal was comparable to or greater than the maser signal and the klystron would lock in on itself and give the appearance of being locked regardless of the frequency to which the klystron was tuned.

In view of the above difficulties, it was thought best to go ahead with the system of Figure 11 until some new filters were procured. New 1N26A crystals were received just as this work was completed which appeared to give better carrier suppression and more sideband power.





This would allow the use of two filters in cascade and should make the system of Figure 10 operable. Another difficulty that was not appreciated at first was the fact that the slightest amount of radiation from the klystron could propagate across the few feet separating it from the balanced mixer with sufficient intensity to cause trouble.

The system of Figure 11 consists of a phase locked klystron which is fed into a balanced modulator where it is amplitude modulated by the low-frequency variable frequency oscillator. The output has the carrier ( $f_0 + 21$ ) suppressed by approximately 20 db with the two sidebands ( $f_0 + \delta$ ,  $f_0 + 42 - \delta$ ) of equal amplitude. This signal is then fed into a filter which passes the desired sideband ( $f_0 + \delta$ ) and attenuates the other sideband and the carrier by 20 to 30 db depending upon the band pass of the filter. A circulator is placed between the klystron and the modulator which provides about 30 db of isolation. Since the two sidebands of the amplitude modulated signal will also propagate down the waveguide towards the klystron, it is necessary to use a directional coupler in the output of the klystron to provide further isolation. A 10 db directional coupler with a directivity of 40 db gives sufficient attenuation to the two sidebands propagating towards the klystron to isolate the mixer from the sideband frequencies. Using 1N26A crystals, an output of up to 0.5 milliwatts was obtained over the frequency range of the system which was a little over two megacycles per second above and below the maser signal  $f_0$ .

The system of Figure 11 has two advantages over the other systems that make it somewhat more desirable. The first of these advantages (which may sound like making a virtue of necessity) is that the desired





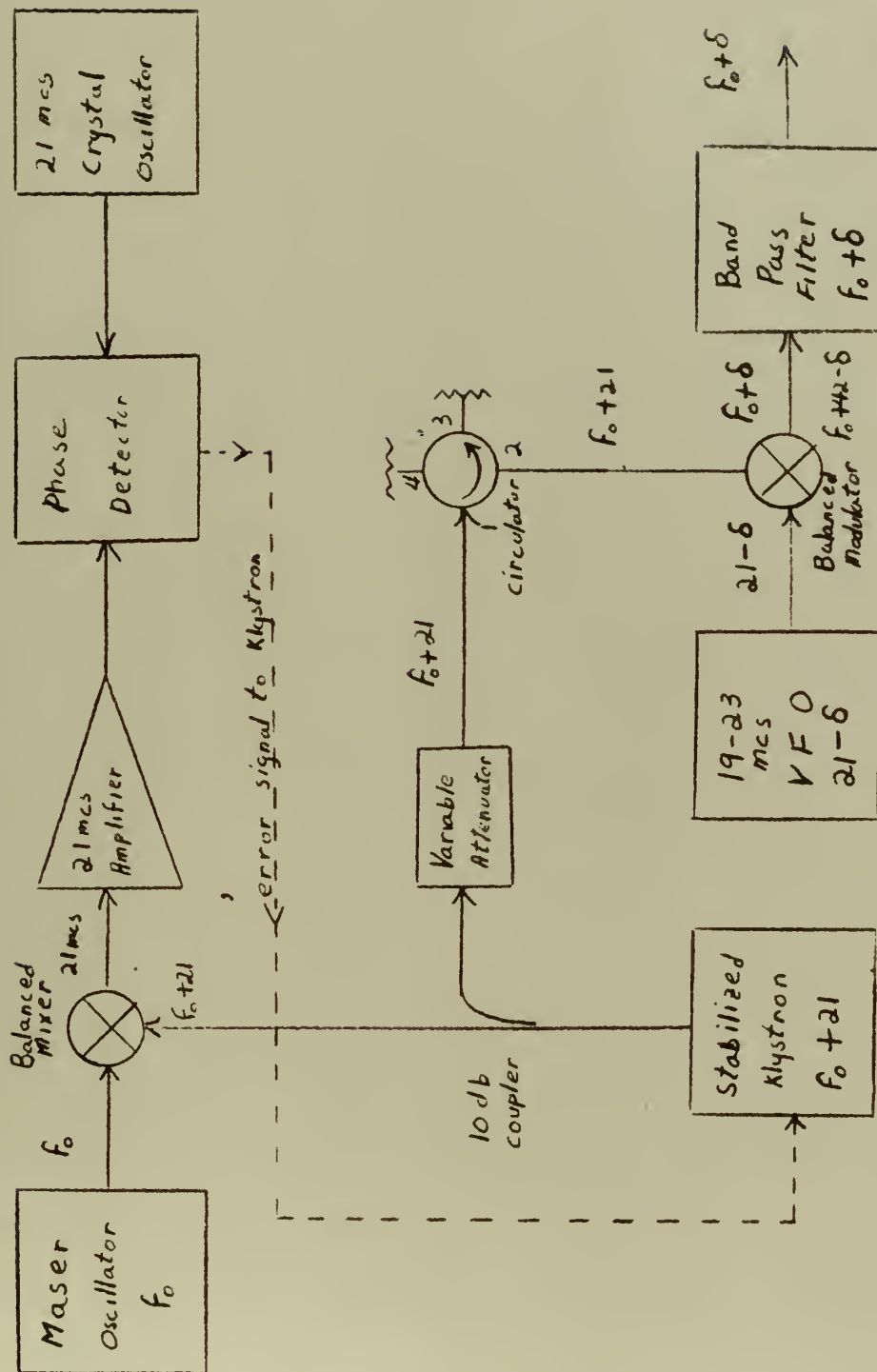


Figure 11. Heterodyne method for obtaining  $f_0 + \delta$



signal is at a relatively low level (less than 0.5 milliwatt) which is very desirable later for measuring the gain versus frequency characteristics of a maser amplifier as well as eliminating some of the shielding problems that arise when there are sizeable powers at or near maser frequency. The second advantage is one of convenience when operating the system. When the klystron is phase locked, the signal going through the i-f amplifier is a very pure signal at twenty one megacycles per second but becomes very cluttered and noisy when unlocked due to the random drifting of the klystron. If a sample of the output of the i-f is fed into a conventional communications receiver with the B F O on, a very pure tone will be heard when the klystron is locked and only noise will be heard when unlocked. Another and less irritating method of determining if the klystron is locked is to turn the B F O off, the automatic gain control on, and the r-f gain to maximum. Now if the klystron is locked, the signal is strong enough to saturate the receiver and the avc cuts the volume to the point where the receiver output is very quiet; but if the klystron breaks lock, the receiver is no longer saturated and the volume goes up to the point where there is considerable noise output. With the klystron locked at a single frequency, it is possible to tell quite easily when it is locked. In the system of Figure 8, the i-f frequency of the second loop is changed as the klystron frequency is changed which requires retuning the receiver each time the frequency is changed if this method is used for insuring that the klystron is phase locked.

The frequency of the signal generator was determined by measuring the frequency of the variable frequency oscillator ( $21 + \delta$  mcs) and subtracting this from the crystal oscillator frequency (21 mcs) to give



the frequency  $\delta$  . By beating the two low-frequency oscillators together and using the difference, drifts in either low-frequency would not matter as this would give  $\delta$  directly and could be added directly to the maser frequency to give  $f_0 + \delta$  . The later method was not used but it would give better accuracy if this were called for.





## 5. Cavity Measurements

One problem frequently encountered in maser construction is the design and testing of cavities to be used in the masers. In general,  $Q$  measurements are rather crude and difficult to make at these frequencies due to the lack of a stable frequency source. A stable tunable frequency source such as the one described in Section 4 makes it possible to make some very precise  $Q$  measurements and should be a very valuable tool for testing new cavity designs.

Before going into the techniques used for measuring the  $Q$  of a cavity, it might be well to review some of the fundamental relationships used in  $Q$  determinations. Figure 13 is an equivalent circuit for a resonant cavity which will be referred to in defining some of the quantities in the following analysis and in Appendix II. The unloaded  $Q$ ,  $Q_0$  is defined as:

$$1) \quad Q_0 = \frac{\omega_0 L}{R} = \frac{1}{\omega_0 C R}$$

The loaded  $Q$ ,  $Q_L$  is defined as:

$$2) \quad Q_L = \frac{\omega_0 L}{R + Z_0} = \frac{Q_0}{1 + Z_0/R}$$

where  $Z_0$  is the impedance seen at the terminals of the cavity which will be assumed to be matched and resistive. The coupling parameter  $b$  is defined as  $b = Z_0/R$  which when substituted into equation 2 gives:

$$3) \quad Q_L = \frac{Q_0}{1 + b}$$

The external  $Q$  of the circuit  $Q_e$  is defined as:

$$4) \quad Q_e = Q_0/b$$



In terms of  $Q_0$ , equation 3 can now be written as:

$$5) \quad \frac{1}{Q_L} = \frac{1+b}{Q_0} = \frac{1}{Q_0} + \frac{1}{Q_e}$$

A technique for determining the loaded  $Q$  and the coupling parameter is described in Chapter 5 of Montgomery<sup>17</sup>. This technique consists of making a series of VSWR measurements as the frequency is shifted through the cavity resonance. A plot is then made of VSWR versus frequency which will be a parabola with the minimum VSWR at resonance and increasing on either side of this center frequency.

One well known definition for the VSWR of a transmission line or wave guide is:

$$6) \quad \text{VSWR} = r = \frac{|Z+Z_0| + |Z-Z_0|}{|Z+Z_0| - |Z-Z_0|}$$

Where  $Z_0$  is the characteristic impedance of the line and is resistive, and  $Z$  is the impedance at the terminals of the line and in general is a function of frequency.  $Z$  can be expressed as:

$$7) \quad Z = R + jX = R + j(\omega L - \frac{1}{\omega C})$$

At resonance there are planes in the line at which  $X = 0$  and equation 6 reduces to:

$$8) \quad r_0 = R/Z_0 = \frac{1}{b}$$

At the half power points,  $|X| = R + Z_0$  which when substituted into equation 6 gives:

$$9) \quad r_1 = \frac{1+b + \sqrt{1+b^2}}{1+b - \sqrt{1+b^2}}$$

After the curve is plotted, the minimum value of the VSWR,  $r_0$ , is obtained and substituted into equation 9 to give the value for  $r_1$ , the VSWR at the half power points. The frequencies at the two half-power



points,  $f_1$  and  $f_2$ , are then obtained from the curve and this is used to determine the  $Q$  from the usual definition for the  $Q$  of a circuit in terms of the half power frequencies and the center frequency:

$$10) \quad Q_L = \frac{f_0}{f_2 - f_1}$$

The above expression for  $Q_L$  is related to the unloaded  $Q$  by equation 5. As yet, no determination has been made to see if  $R$  is greater or less than  $Z_0$ . This determination is described in Montgomery and will not be covered here.

The method described above is limited to cases where the signal source can be tuned in frequency over a range that is large enough to cover the half-power points of the loaded cavity. The total bandwidth of the signal source as described in Section 4 was approximately four megacycles which put a lower limit of around 6000 as the minimum loaded  $Q$  that could be measured with the set up without extrapolating the curve. It is however, just those cavities in which  $Q$  is large where previous techniques were least satisfactory and where the present instrument is of greatest value. To allow the use of the system for cavities with lower values of  $Q_L$ , a more general derivation in terms of a parameter  $a$  is included in Appendix II. The results of this appendix are listed below:

$$11) \quad r_a = \frac{1 + b + \sqrt{1 + b^2 - 2b\left(\frac{1-a^2}{1+a^2}\right)}}{1 + b - \sqrt{1 + b^2 - 2b\left(\frac{1-a^2}{1+a^2}\right)}}$$

$$12) \quad Q_L = \frac{a f_0}{f_2 - f_1}$$

When  $a$  is one, equations 11 and 12 reduce to equations 9 and 10.

Rather than eliminate  $a$  from equations 11 and 12, it was found





simpler to choose a value for  $a$  and try it and readjust if necessary. With a four megacycle per second frequency range, a choice of  $a$  as 0.5 is generally sufficient to cross the curve except for cavities with extremely low loaded  $Q$ 's.

Figure 12 is a block diagram of the apparatus used for making  $Q$  measurements on several experimental cavities using the techniques described above. The signal was amplitude modulated at one kilocycle per second with a ferrite gyroline which made it possible to use a sensitive detector such as a HP 415B standing wave indicator. For precision measurements, the VSWR was determined by using the precision attenuator and a constant meter deflection rather than the VSWR indication of the meter. It is very important that an isolator be placed between the gyroline and the slotted line as the impedance of the gyroline changes considerably while modulating the r-f signal.

A typical plot made from data taken on an experimental maser cavity is shown in Figure 14. Other measurements are tabulated in Table II along with some of the parameters used in the measurements. No cavities were available with values of  $Q_o$  greater than 10,000 which would have given the system a much better test but the results of the measurements made indicate that the system has considerable merit even with loaded  $Q$ 's of a few thousand.

TABLE II

Cavity	$r_o$	$r_{\frac{1}{2}}$	$b$	$Q_L$	$Q_o$	$Q_e$
A	1.075	2.62	1.075	3060	6340	5900
B	7.5	9.93	0.133	7800	8840	66,300
C	6.3	8.45	0.159	7750	8990	56,600

Results of typical cylindrical cavity  $Q$  measurements with measured and calculated parameters.





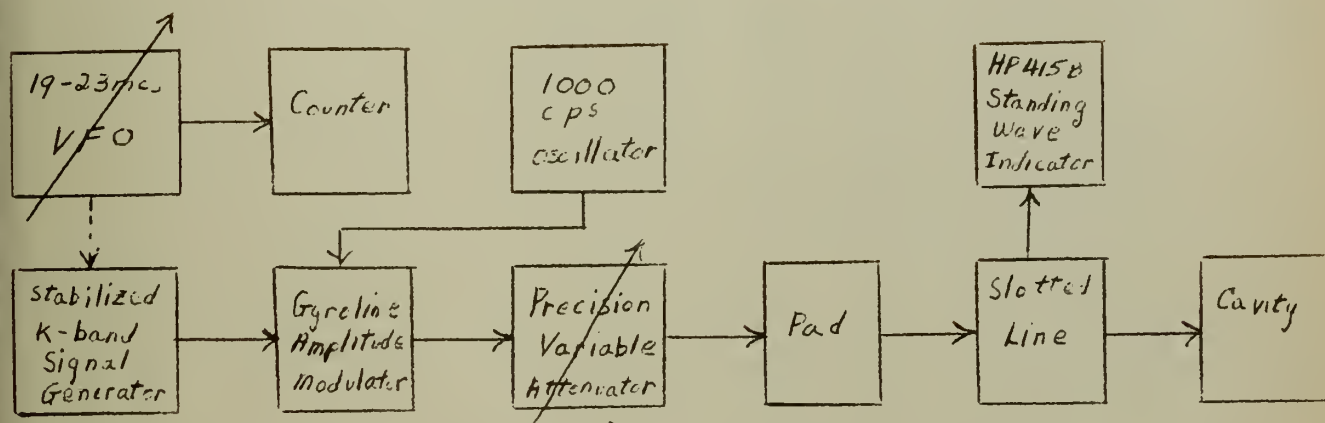


Figure 12. Block diagram of apparatus used for Q measurements.

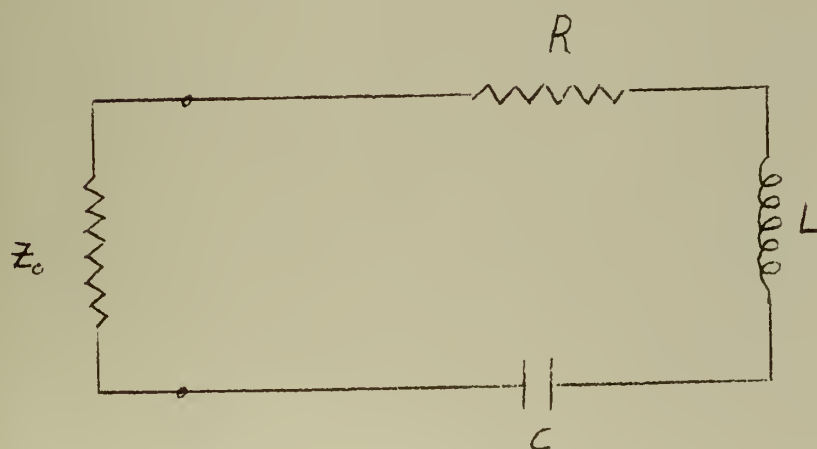


Figure 13. Equivalent circuit for a microwave cavity.





Determination of  $Q_L$  of cavity B (Table II)

$$\delta = f - f_m \quad f_2 - f_1 = \delta_2 - \delta_1$$

$$f_m = 23870.131 \text{ mcs}$$

$$f_0 = f_m + \delta_0$$

$$Q_L = \frac{f_0}{f_2 - f_1} = \frac{23871.012}{1.69} = 0.16$$

$$Q_L = 7800$$

$$n_0 = 7.5$$

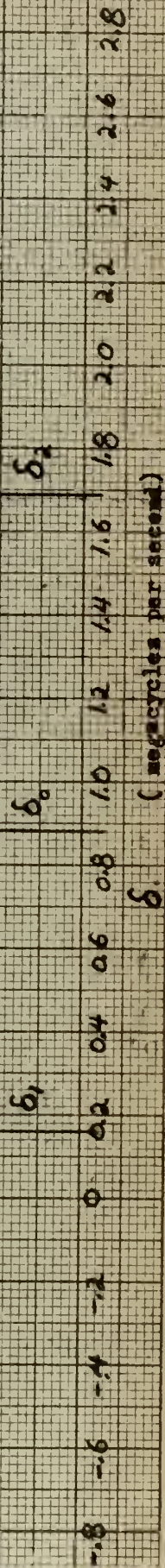


Figure 14. Plot of VSWR vs frequency for determining  $Q$  of a microwave cavity.





## 6. Maser Gain Measurements Using the Stabilized Signal Generator

One of the reasons for construction of the stabilized K-band signal generator was to provide a signal that could be used to measure the gain of a maser amplifier as a function of frequency. The narrow bandwidth of a beam maser requires the measurements be made over a range of several hundred cycles. This is impractical with conventional K-band signal generators which might drift several kilocycles while a measurement is being made.

Theory predicts that a beam maser might typically have a midband gain of up to thirty db with a half-power bandwidth of approximately one kilocycle per second. This means that the gain measurements should be spaced no further apart than 100 cycles and preferably closer near the half-power points. Theory further predicts that nonlinearities in the amplifier will cause saturation at a power level of  $10^{-10}$  watts or -70 dbm. Thus the gain measurements must be made at a very low level ~~this~~ <sup>that</sup> is below the saturation level of the amplifier.

A modified Dicke radiometer was available which would provide a sensitive detector for the measurements. It was felt that the radiometer would be the most desirable type of detector to use although other methods could have been used. The Dicke radiometer is discussed in more detail in Appendix II.

The system for making the gain measurements is shown in Figure 15. For the purposes of the measurements, the signal generator output is set at 0.1 milliwatt and held constant. Another 60 db of attenuation is then inserted through the use of two 30 db couplers. The power level of the signal into attenuator number one is thus -70 dbm. The signal out of





the attenuator is divided and sent into the two arms as shown in the figure. The signal in the upper arm goes through a precision attenuator and then to terminal No. 2 of the chopper. The signal in the lower arm goes through a precision attenuator and into terminal one of a ferrite circulator. The circulator and maser cavity together comprise the maser amplifier. Terminal two of the circulator is connected to the maser cavity, terminal three goes to terminal No. 2 of the chopper, and terminal four is terminated in a matched load. The chopper output goes on to the remainder of the radiometer.

The system is initially zeroed by removing the maser amplifier and placing a short circuit between points A and B. Attenuator number one is then adjusted to insure that the power level into the two arms is well below -70 dbm. After this the precision attenuators in the two arms are adjusted for a null reading of the radiometer and the readings noted. The circulator and maser are then reinserted into the system and the measurements can be made.

With the amplifier in the loop, it will be necessary to readjust the attenuator in the lower arm to obtain a null reading on the radiometer. The difference in the initial and the final readings on this attenuator will then be the gain between points A and B. To determine the gain of the maser with a perfect lossless circulator it is necessary to determine the attenuation between points A and B with a short at the input terminals of the maser and add this to the gain of the maser amplifier.

Preliminary tests of the above system indicate that the gain between points A and B can be determined to within 0.25 db at a power



level of -85 dbm and a system bandwidth of two megacycles per second. A narrower bandwidth would provide better sensitivity but the accuracy of the precision attenuator is limited to about 0.25 db.

Time did not permit making the series of gain measurements on the maser amplifier due to difficulties encountered with the maser amplifier but preliminary tests indicate that the system described will be more than adequate. Dr. Stitch's group at Hughes should be making a series of gain measurements using this technique in the near future. These measurements together with other noise measurements will then be used in computing the noise temperature of the beam maser amplifier.



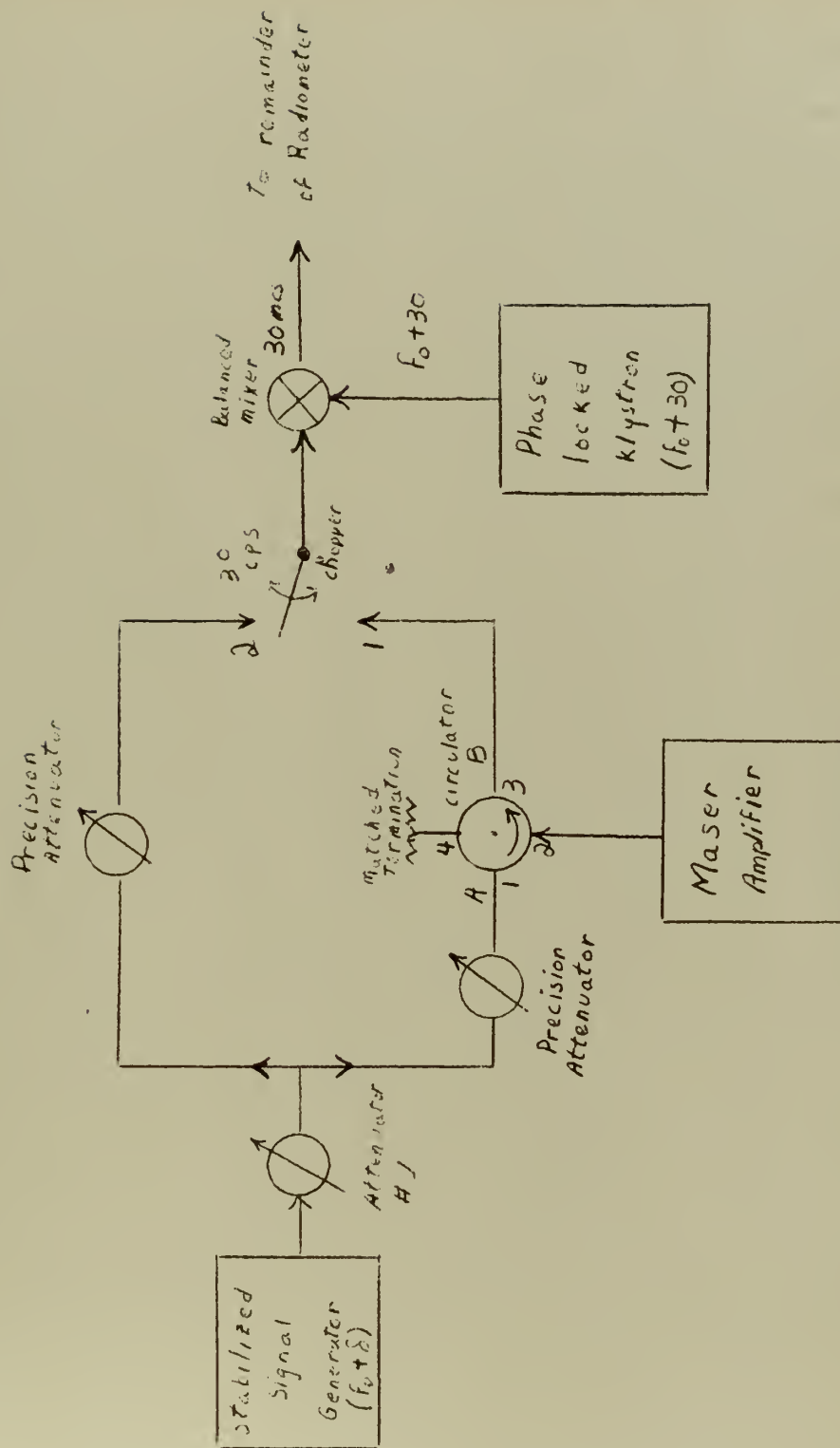


Figure 15: Block diagram of gain measuring apparatus.



## 7. Conclusion

In section one, the stability of maser oscillators was discussed and it was pointed out that short time stabilities as great as one part in  $10^{13}$  have been obtained. Long time stabilities of one part in  $10^{10}$  are readily obtained without any great sophistication in the construction of the maser. Bonanomi is doing work with a dual cavity that may give a stability of one part in  $10^{12}$  over long periods of time.<sup>18</sup>

In order to study the characteristics of maser cavities such as the one designed by Bonanomi, it is necessary to have a stable signal generator near the frequency of the maser signal. To make any measurements of the gain of a maser amplifier, it is necessary to have a stable signal at the precise center frequency of the maser pass-band and preferably one that can be tuned above and below this frequency. To meet both these requirements, a maser stabilized signal generator was constructed that could be tuned approximately two megacycles per second above and below the maser signal frequency.

The signal generator was constructed using a phase locked klystron loop as described in sections three and four. The first system attempted did not work as expected due to not having an efficient balanced modulator and filtering arrangement. The experimental work that was performed with this system did indicate that a very slight improvement in the modulator and filter should make it operable. The second system attempted worked quite well and was relatively easy to line up and operate. The power output was approximately one half milliwatt over the frequency range and was sufficient for the cavity and gain measurements.





The signal generator described in section four was used to measure the  $Q$  of three experimental cavities to within five percent. Better results could have been achieved using the system but this was not required for the cavities that were measured. The frequency range of the signal generator was limited to about four megacycles which restricts its use with conventional techniques to cavities with loaded  $Q$ 's of 6000 or greater where the greatest measurement problems exist. To eliminate this limitation, a technique for obtaining  $Q$  measurements on cavities with low loaded  $Q$ 's is developed in Appendix I.

A system for measuring the gain of a maser amplifier is described in section six. Preliminary tests on the system indicate that it will work quite well for the gain measurements. Difficulties encountered with the maser amplifier prevented the writer from performing the gain measurements but these should be made in the near future using the system described.

Several other applications for a stable signal generator such as this appear to be quite promising and should warrant further investigation. One such application will be described in some detail and a few others will be mentioned briefly.

Figure 16 is a block diagram showing one method for obtaining a stable X-band carrier for a microwave transmitter. A transmitter of this sort would be well suited for a satellite communication system such as that proposed by Pierce and Kompfner.<sup>19</sup> One objection to communication links at these frequencies is the difficulty in obtaining a stable signal. Another difficulty encountered is that of



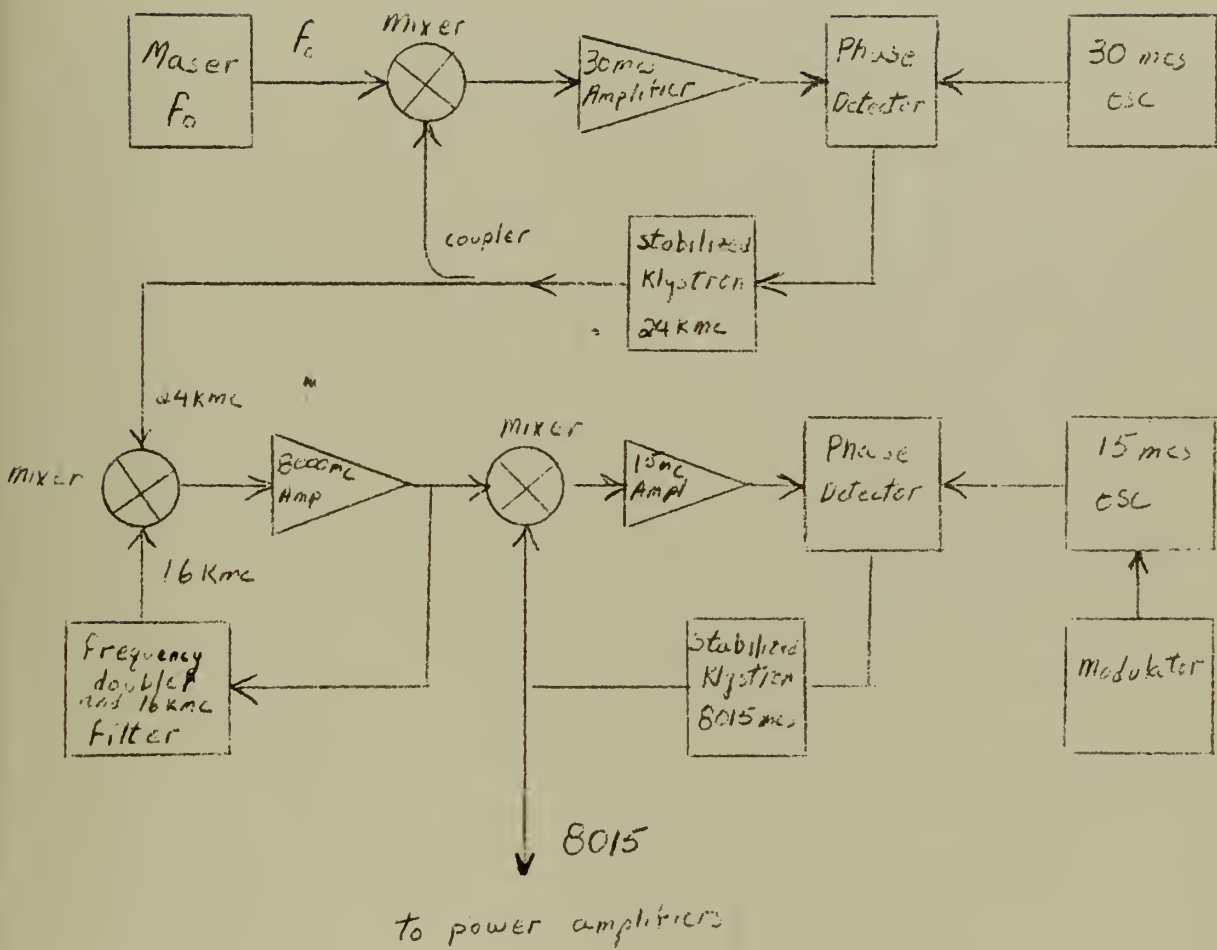


Figure 16 A method for obtaining a stable 8000 mcs signal.



efficiently and effectively modulating microwave signals.

The system shown in Figure 16 consists of a phase locked klystron such as that shown in Figure 6. For simplicity, it will be assumed that the klystron is stabilized at 24,000 megacycles per second rather than 23,900 megacycles per second. The output of this klystron is fed into a regenerative divider feedback loop which will have an output of 8000 megacycles per second with the same stability as the 24 kilo-megacycles per second klystron. This stable 8000 megacycles per second signal is then used as the reference signal for another phase lock loop to stabilize a klystron at 8015 megacycles per second. The output of the klystron then goes to the final power amplifiers. Many other schemes could be used.

A block labeled modulator is shown in Figure 16 feeding the 15 megacycles per second reference oscillator of the second phase detector. This could be used to frequency or phase modulate the reference oscillator and this modulation would then be impressed upon the carrier. For a high speed digital transmission system, this modulation would be easy to accomplish. Existing transmitter master oscillators such as the one in the AN/FRT-17 could be used as the 15 megacycles per second reference oscillator in this system. This would then permit use of the associated frequency shift keying equipment for digital transmission.

A system such as the one just described if modified slightly would be compatible with many of the newer communications systems such as the Collins Kineplex system. Coherent detection techniques could be used if a comparable signal generator was available at the receiving end.





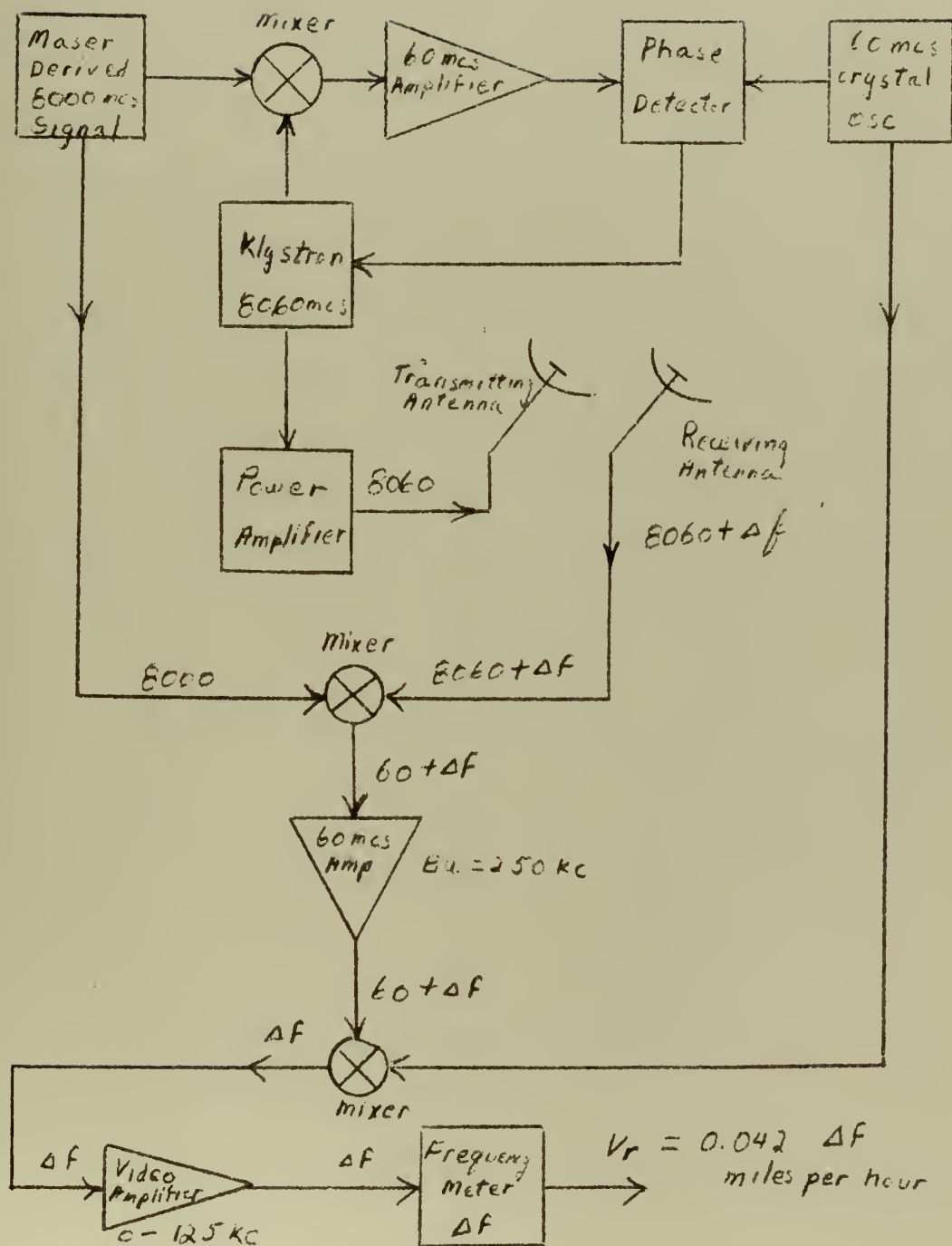


Figure 17. Maser stabilized C-W radar.



A simple block diagram of a Doppler radar using a maser stabilized klystron is shown in Figure 17. In this system, a stable 8060 megacycles per second signal is provided as in the previous scheme which is fed into a power amplifier which feeds the tracking antenna. The returning signal will be at a frequency of 8060 megacycles per second plus some small frequency displacement  $\Delta f$  for a target that is approaching the radar. The magnitude of  $\Delta f$  is given by  $(2v_r/c)f$  where  $v_r$  is the radial velocity of the target,  $c$  is the velocity of light and  $f$  is the radar frequency.<sup>20</sup> This signal from the receiving antenna is mixed with the 8000 megacycles per second signal to give an i-f signal that is amplified and then mixed with the signal from the 60 megacycles per second oscillator to obtain  $\Delta f$ . This value of  $\Delta f$  is then a direct indication of the targets radial velocity. For an 8060 megacycles per second signal, the radial velocity is given by:

$$13) \quad v_r = 0.042 \Delta f \text{ miles per hour}$$

Arbitrarily picking a value of 5000 miles per hour as an upper limit for velocities to be detected, the maximum value of  $\Delta f$  turns out to be 119 kilocycles per second. Thus the system bandwidth need be only 238 kilocycles per second. Using a 60 megacycles per second crystal oscillator with a short time stability of one part in  $10^7$ , the maximum error in the velocity would be less than 0.5 miles per hour over the range and would in general be much better as the oscillator would not drift an appreciable amount during the time between transmission and receipt of the signal.

Recent advances in high-power klystron amplifiers and traveling wave tubes make it possible to use a stable signal of this sort in a pulsed



radar system which would provide both range and velocity. Since all of the signals are derived from the same oscillators, there would be no difficulty with coherence of the signals and moving target indicators would be relatively simple to build.

Using various combinations of phase detector loops and regenerative feedback loops, the entire frequency spectrum could be covered in steps to obtain stable signals where needed. The addition of a variable frequency oscillator into one or more of the phase lock loops would allow continuous tuning over limited ranges. Using techniques of this sort, a frequency standard covering the frequency spectrum could be constructed.

Generally speaking, a stable K-band signal generator of the type discussed in this paper makes it possible to use many of the techniques that are normally restricted to the lower frequencies. Measurements on various components can be made with much greater precision, frequency meters can be precisely calibrated, high-Q devices can be studied much more closely, receiver bandwidths can be reduced as well as many other things that have been either difficult or impossible in the past. Microwave communications would become similar to lower frequency communications in many respects with stable signal generators available.





## BIBLIOGRAPHY

1. J. P. Gordon, H. J. Zeiger and C. H. Townes, "The maser -- new type of microwave amplifier, frequency standard, and spectrometer," *Phys. Rev.*, vol. 99, pp. 1264-1274; August, 1955.
2. H. Lyons, "Atomic Clocks," *Scientific American*, Vol. 196, February, 1952
3. W. Higa, "Observations of Nonlinear Maser Phenomena," *Review of Scientific Instruments*, vol. 28, p. 726, 1957
4. R. W. Damon, "Maser shows promise, some drawbacks" (Pt. I), and "Maser's potential rests on further work" (Pt. II), *Aviation Week*, pp. 76-89; August 19, 1957 and pp. 91-104; August 26, 1957.
5. J. P. Wittke, "Molecular amplification and generation of microwaves," *Proc. IRE*, vol. 45, pp. 291-316; March, 1957.
6. J. C. Helmer, "Theory of a molecular oscillator," Stanford Univ., Stanford, Calif., Microwave Lab. Rep. No. 311; June, 1956
7. H. Heffner, "Solid State Microwave Amplifiers," *IRE Transactions on Microwave Theory and Techniques*, vol. MTT7, pp. 83-91, January, 1959.
8. Wright and Randall, *Phys. Rev.*, vol. 44, pp. 391, 1933
9. Cleeton and Williams, *Phys. Rev.*, vol. 45, p. 234, 1934
10. R. V. Pound, *Rev. Sci. Inst.* vol. 17, p. 490, 1946
11. Smith, Quevedo, Carter, and Bennett, *J. Appl. Phys.*, vol. 18, P. 1112, 1947
12. Lamont and Hicken, *Brit. J. Appl. Phys.*, vol 3, p. 182, 1952
13. H. Lyons, *Ann N.Y. Acad. Sci.*, vol. 55, p. 831, 1952
14. K. J. Shimoda, *Phys. Soc. Japan*, vol. 9, p. 378, 1954
15. M. Peter and M. W. P. Strandberg, "Phase Stabilization of Microwave Oscillators," *Proc. IRE*, vol. 43, pp. 869-873, July, 1955
16. E. F. Davis, "Phase Stabilization to Microwave Frequency Standards," *Jet Propulsion Lab. External Publication*, No. 380, June, 1957
17. C. G. Montgomery, *Technique of Microwave Measurements*, MIT Radiation Lab. Series, vol. 11, McGraw Hill, 1947.
18. J. Bonanomi, "Maser Research at Neuchatel Univ., Switzerland," *Proc. of 12th Annual Symposium on Frequency Control*, pp. 538, 1958
19. Pierce and Kompfner, "Transoceanic Communication by Means of Satellites," *Proc. IRE*, vol. 47, pp. 372-380, March, 1959





20. L. N. Ridenour, Radar System Engineering, MIT Radiation Lab. Series, vol. 1, p. 128, McGraw-Hill, 1947
21. R. H. Dicke, "Measurement of Thermal Radiation at Microwave Frequencies," Rev. of Sci. Inst., vol. 17, July, 1946
22. A. E. Siegman, "Gain-bandwidth and noise in maser amplifiers," Proc. IRE, vol. 45, p. 1737; December, 1957
23. M. L. Stitch, "Maser amplifier characteristics for transmission and reflection cavities," J. Appl. Phys., vol. 29, pp. 782-789; May, 1958
24. J. C. Helmer, "Theory of a molecular oscillator," Stanford Univ., Stanford, Calif., Microwave Lab. Rep. No. 311; June, 1956
25. K. Shimoda, T. C. Wang, and C. H. Townes, "Further aspects of the theory of the maser," Phys. Rev., vol. 102, pp. 1308-1321; June, 1956
26. C. H. Townes, "Comments on frequency-pulling of maser oscillators," J. Appl. Phys., vol. 28, pp. 920-921; August, 1957
27. J. C. Helmer, "Maser oscillators," J. Appl. Phys., vol. 28, pp. 212-215; February, 1957
28. J. C. Helmer and M. W. Muller, "Calculation and measurement of the noise figure of a maser amplifier," IRE Trans. on Microwave Theory and Techniques, vol. MTT-6, pp. 210-214; April, 1958
29. W. H. Wells, "Maser oscillator with one beam through two cavities," J. Appl. Phys., vol. 29, pp. 714-717; April, 1958



## APPENDIX I

### Cavity Q Measurements From VSWR Measurements

The derivation to follow is for the loaded Q of a resonant microwave cavity. If the quantity  $(R + Z_0)$  is replaced by R throughout the derivation, the results will be valid for the unloaded Q of the cavity. The relations between  $Q_0$ ,  $Q_L$ , b and  $Q_e$  are given in section 5 of this report.

Figure 13 is an equivalent circuit for a resonant microwave cavity that is valid near resonance when the circuit can be represented by a series resonant circuit. The impedance of the circuit is given by:

$$1) \quad Z = R + jX \quad \text{where } X = (\omega L - 1/\omega C)$$

at resonance,  $\omega_0 L = 1/\omega_0 C$  and  $X = 0$

For the idealized circuit of Figure 11, the response curve can be considered to be symmetrical and centered about  $f_0$ .

There will exist two frequencies  $f_1$  and  $f_2$  such that:

$$2) \quad 1/\omega_1 C - \omega_1 L = a(R + Z_0) \quad \text{where } \omega_1 = 2\pi f_1$$

$$3) \quad \omega_2 L - 1/\omega_2 C = a(R + Z_0) \quad \text{where } \omega_2 = 2\pi f_2$$

Where  $a$  is a parameter that can be adjusted to make best use of the data available. When  $a$  is one,  $f_1$  and  $f_2$  are the half power frequencies. If the best data is near  $f_0$ ,  $a$  should be chosen to be less than one.

Solving 2 and 3 for LC:

$$4) \quad LC = \frac{1 + a\omega_2 C(R + Z_0)}{\omega_2^2} = \frac{1 - a\omega_1 C(R + Z_0)}{\omega_1^2}$$

The loaded Q,  $Q_L$  is given in terms of the circuit parameters by:

$$5) \quad Q_L = \frac{1}{\omega_0 C(R + Z_0)} = \frac{\omega_0 L}{R + Z_0}$$



Solving equation 5 for  $C(R+Z_0)$  and substituting into 4 gives:

$$6) \left(1 + \frac{a\omega_1}{\omega_0 Q_L}\right) \omega_1^* = \left(1 - \frac{a\omega_1}{\omega_0 Q_L}\right) \omega_1^2$$

Simplifying and solving for  $Q_L$ :

$$7) Q_L = \frac{a\omega_1 \omega_1}{\omega_0(\omega_2 - \omega_1)} = \frac{af_1 f_2}{f_0(f_2 - f_1)}$$

With a symmetrical response curve,  $f_1 = f_0 - \delta$  and  $f_2 = f_0 + \delta$

so that  $f_1 f_2 = f_0^2 - \delta^2$  which can be approximated by  $f_0^2$

for  $f_0$  much greater than  $\delta$ . Thus equation 7 reduces to:

$$8) Q_L = \frac{af_0}{f_2 - f_1} = \frac{af_0}{2\delta}$$

The VSWR for the circuit of Figure 11 is given by:

$$9) r = \frac{|Z+Z_0| + |Z-Z_0|}{|Z+Z_0| - |Z-Z_0|}$$

where  $Z$  is the circuit impedance as defined by equation 1.

For the case when  $Z_0$  is a pure resistance, equation 9 becomes:

$$10) r = \frac{\sqrt{(R+Z_0)^2 + X^2} + \sqrt{(R-Z_0)^2 + X^2}}{\sqrt{(R+Z_0)^2 + X^2} - \sqrt{(R-Z_0)^2 + X^2}}$$

At the frequencies  $f_1$  and  $f_2$ ,  $X = a(R+Z_0)$ . The VSWR is then given by:

$$11) r_a = \frac{\sqrt{(R+Z_0)^2 + a^2(R+Z_0)^2} + \sqrt{(R-Z_0)^2 + a^2(R+Z_0)^2}}{\sqrt{(R+Z_0)^2 + a^2(R+Z_0)^2} - \sqrt{(R-Z_0)^2 + a^2(R+Z_0)^2}}$$

When  $a$  is zero, the above expression reduces to:

$$12) r_0 = Z_0/R = b \quad \text{for } Z_0 > R$$

$$\text{or } r_0 = R/Z_0 = 1/b \quad R > Z_0$$





Equation 11 can be simplified to the following expression:

$$13) \quad r_a = \frac{1+b + \sqrt{1+b^2 - 2b\left(\frac{1-a^2}{1+a^2}\right)}}{1+b - \sqrt{1+b^2 - 2b\left(\frac{1-a^2}{1+a^2}\right)}} \quad Z_o > R$$

$$r_a = \frac{1+\frac{1}{b} + \sqrt{1+\frac{1}{b^2} - 2b\left(\frac{1-a^2}{1+a^2}\right)}}{1+\frac{1}{b} - \sqrt{1+\frac{1}{b^2} - 2b\left(\frac{1-a^2}{1+a^2}\right)}} \quad R > Z_o$$

$$14) \quad r_{\frac{1}{2}} = \frac{1+b + \sqrt{1+b^2 - 1.2b}}{1+b - \sqrt{1+b^2 - 1.2b}} \quad a = \frac{1}{2}$$

$$15) \quad Q_L = \frac{\frac{1}{2} F_o}{F_2 - F_1} \quad a = \frac{1}{2}$$

$$16) \quad r_1 = \frac{1+b + \sqrt{1+b^2}}{1+b - \sqrt{1+b^2}} \quad a = 1.0$$

$$17) \quad Q_L = \frac{F_o}{F_2 - F_1} \quad a = 1.0$$



## APPENDIX II

In 1946 R. H. Dicke announced a new type of radiometer for measuring thermal radiation at microwave frequencies.<sup>21</sup> Using this device, Dicke was able to detect very feeble noise powers and very slight fluctuations in noise power. Using a bandwidth of 16 megacycles per second and a time constant of 2.5 seconds, the minimum detectable power for the radiometer is approximately  $2 \times 10^{-21}$  watts per cycle and the minimum detectable noise temperature is less than 0.5 degree Kelvin. Dicke's basic circuit has not changed appreciably over the years although several minor modifications have evolved. The greatest changes have come about in the switching methods and the coherent 30 cycle detector.

The purpose of this appendix is to describe briefly a modified Dicke radiometer to be used at K-band for detecting very narrow band noise out of a maser amplifier. Only a very brief description of the apparatus will be given in order to allow the reader to understand the principle of the system without the distractions of the detailed theory. Dicke gives a very clear picture of the theory and operation of the radiometer in his paper should more details be desired.

Figure 18 gives a block diagram of the apparatus that makes up the radiometer. The general appearance of the signal is shown at several points along the line. For the purposes of this paper, it is assumed that the switch is a perfect one that will switch from the noise source  $T_N$  to the unknown  $T_X$  at a rate determined by the motor driving the switch. Thus the input to the balanced mixer will have a square wave envelope as shown at point b in Figure 18. The noise signal out of the calibrated



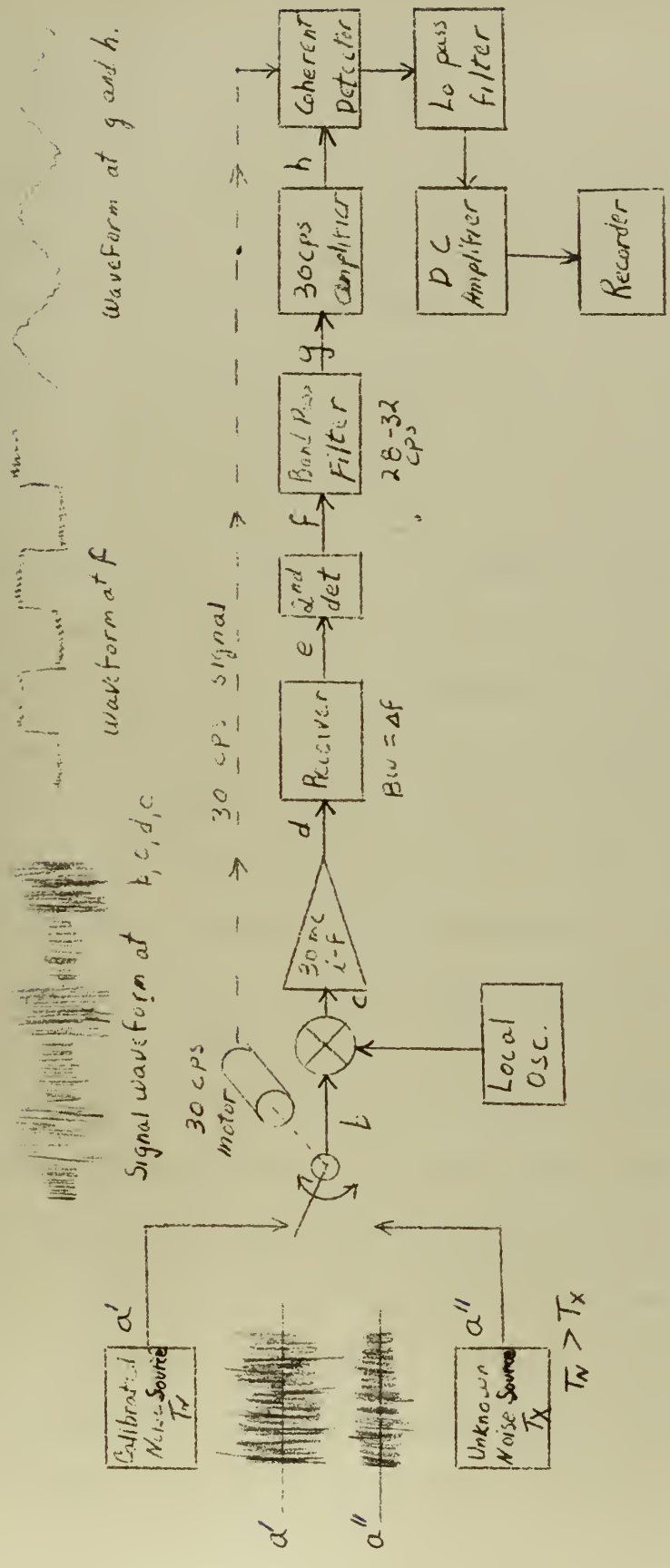


Figure 18. Block diagram of the modified Dicke Radiometer



noise source  $T_N$  is shown at point a' and that of the unknown at point a'' for the case where  $T_N$  is greater than  $T_X$ .

The square wave envelope of the signal at point b will be present in the signal at point c but this will have noise from the local oscillator and the crystal mixer impressed upon it. The components of the signal that fall within the band pass of the i-f amplifier will pass through the amplifier and emerge at point d with the same general square wave configuration. This signal is then sent through a communications receiver such as a H R O where the noise bandwidth is limited by the band-pass of the receiver. At the second detector in the receiver the square wave envelope of the signal is detected and sent through a narrow band filter set to pass the fundamental of the square wave signal. With the motor driving the switch set at 30 revolutions per second, the signal out of the band-pass filter will be a 30 cycle per second sine wave with small amounts of noise impressed upon it. This signal is then amplified and sent into a coherent detector synchronized with the motor driving the switch. The coherent detector reduces the bandwidth to approximately one cycle per second.

The coherent detector is followed by a low pass filter with a time constant of approximately two seconds. This signal is a slowly varying d-c voltage that is amplified and applied to a Brush recorder or d-c meter. If the two sources  $T_N$  and  $T_X$  have the same average power, there will be no change in the amplitude as the switch goes from a to a' and no modulation on the signal going through the system. The signal at the recorder will then be zero except for system noise. As the two





signals change in amplitude, the modulation amplitude changes and the 30 cycle signal changes which results in a change in the d-c level at the recorder.

The ultimate sensitivity of a system of this nature is limited by the unwanted noise that is picked up in the system. The sensitivity of the system is given by:

$$1) \quad \frac{\Delta T}{T_N} = \frac{\pi N'}{8\sqrt{2\tau\Delta f}}$$

where  $\Delta T$  is the minimum detectable temperature difference.

$T_N$  is the temperature of the calibrated noise source.

$N'$  is the noise figure of the receiver standardized to  $T_N$  instead of 290 degrees Kelvin so that  $N' = (N-1) (290/T_N) + 1$ ; where  $N$  is the conventional noise figure

$\tau$  is the time constant of the low pass filter.

$\Delta f$  is the bandwidth of the receiver.

With a bandwidth of 16 megacycles per second, a noise figure of 25 and a time constant of 2.5 seconds, the minimum detectable temperature difference is 0.46 degrees Kelvin at 300 degrees Kelvin.















thesG195

A maser stabilized K-band signal generat



3 2768 002 01061 3

DUDLEY KNOX LIBRARY